Future Generation of Communication and Internet of Things (FGCIOT)

Journal homepage: http://fgciot.semnaniau.ac.ir/

PAPER TYPE (Research paper)

Effect of mechanical sever plastic deformation on corrosion current density and electrochemical impedance of AZ91 magnesium Alloy

Seyed Rahim Kiahosseini[1*], Armin Aminian[1]

[1]Department of Engineering, Damghan Branch, Islamic Azad University, Damghan, Iran.

Article Info

Article History:
Received: 1 November, 2023
Revised: 14 January, 2024
Accepted: 20 February, 2024

Keywords:
Sever plastic deformation; Corrosion; Hardness; Polarization

*Corresponding Author's Email Address:

Abstract

Magnesium alloys have been considered due to its high strength to weight ratio. In this study, cubic samples of as-cast AZ91 were cut in the dimension of $1 \times 1 \times 1$ cm^3, and then a hot severe plastic deformation process was applied on them at 350 °C. The samples were continuously compressed in the direction of x, y and z. The raw samples and one, two and three-directional forged samples were evaluated by Vickers hardness, potentiodynamic polarization, scanning electron microscopy (SEM), and electrochemical impedance methods. Vickers hardness evaluation showed that by applying forging in three continual directions, the hardness of the raw sample increased from 74 HV to 86 HV. However, by increasing the number of forging pass, the corrosion current density decreased from 2 mA/cm^2 to about 6.9 $\times 10^{-4}$ mA/cm^2. SEM evaluation indicated that corrosion zones were reduced by increasing deformation. Polarization resistance obtained from electrochemical impedance method increased from 381.99 to 1914.4 $\Omega.cm^2$ related to the as-cast and three-directional deformed samples, respectively. The event confirmed that anodic regions reduced on the surface of forged samples. The mentioned results confirmed the positive effect of grain size reduction, applied compressive strength and blocking of the presented micro-voids on the corrosion behavior of the alloy.

INTRODUCTION

According to the high strength to weight ratio of magnesium alloy that decreases energy consumption, the alloyis a low-weight metal widely used in different engineering application such as automobile manufacturing, sport, and electronic industries[1-3]. Nevertheless, the presence of limited slip systems in magnesium alloys results in their low deformability in ambient temperature. Hence, it is required to develop applying new magnesium-based materials due to its acceptable mechanical properties[4-7]. Although the most proportion of commercial magnesium alloys is produced by the casting methodology, the contribution of as-cast magnesium alloys in the whole applications of magnesium alloys is lower than 10% [8].

Many activities in the field of mechanical refinement of magnesium alloys have been performed to develop the applications of the alloys in automobile manufacturing and aerospace industries. In the past decades, many mg alloy systems have been developed, such as az system, zk system, we system, etc[9-12].

Scientists have been developed high strength magnesium alloys by improving properties of commercial alloys[13-15]with applying different mechanical and metallurgical processes, which result in optimizing grain size and improving strength by precipitation strengthening method[16, 17]. For example, a high strength mg-y-zn alloy, produced by powder metallurgy method, indicated outstanding mechanical properties, including tensile yield strength (tys) of 610 mpa and an elongation of 5%[18].

Doi:

One of the most critical parameters in the development of magnesium alloy properties is high-temperature forming. Actually, during hot forming of magnesium alloys, because of their stacking fault energy (sfe) that is about 125 mj/m2, dynamic recovery phenomenon occurs that influences softening and grain size of the alloy[19, 20].

Deformed magnesium alloys are considered more than as-cast ones due to their higher mechanical properties. Besides, lower porosity is observed in the deformed alloys, and corrosion behavior of the alloys is outstanding. Limited studies have been done on the corrosion behavior of magnesium alloys[21, 22].

From advanced processes that can modify the microstructure and improve mechanical properties of magnesium alloys, severe plastic deformation such as hot extrusion, equal-channel angular processing, etc. Can be mentioned[23]. Dynamic recrystallization, occurs in the whole of the sample by applying hot severe plastic deformation, causes the formation of an acceptable microstructure[24, 25].

According to various researches, severe plastic deformation (spd) can modify the grain size of large solids in submicron or nanometer level[26]. Among spd procedures multi-axial forging, its potential is considered because of its ability to apply in industrial applications and produce large-scale samples[27, 28]. Because the shape of the material is not affected by multi-axial forging, the thickness and diameter reduction appeared in rolling and extrusion processes are not observable in the forging method. Due to high temperature and low compressive stress applying during multi-axial forging, the process can be used upon brittlematerials[29-35].

EXPERIMENTAL

In this study, az91 magnesium alloy (mg-9.3% al-0.96% zn-0.14% mn), cast in the sand, was used andcubic samples with the dimension of $1 \times 1 \times 1$ cm3 were cut from as-cast alloy, homogenized at 420 °c for 24 h, and then quenched in water.

In order to apply hot deformation process on the samples, each sample was heated up to 350 °c at a furnace with hot argon atmosphere, and then quickly transferred to a 25-ton press instrument (zwick/roll) to apply compression process with the strain rate of 0.1 s-1 until real strain received to 0.3. Four types of the samples were assessed including an as-cast raw sample and other three types that compressed in the direction of x, the direction of x and y, and the direction of x, y and z, respectively.

To evaluate the hardness of the samples, the vickers hardness method was used. For this purpose, a 3-kg force was applied on a sample with a pyramid indenter with the angle of 136°, then the average diameter of the projected area of the indenters (d) was determined by optical microscopy and hardness was calculated by equation (1)[36].

$$H_V = \frac{1.8544F}{D^2} \quad (1)$$

To assess the corrosion behavior of the samples, potentiodynamic polarization method in a solution containing 3.5% nacl was used, and a saturated calomel electrode as a reference electrode was considered. Before the test, the samples were immersed in the solution for 1 h to obtain electrochemical equilibrium. Then, the test was done in the voltage range of -0.4 to 0.4 mvref and the open circuit potential range with the scan rate of 1 mv/s.

For investigation of grains, the samples were etched in nital solution for 30 seconds and the used an optical microscope. The morphology and corroded surface of the samples were studied via scanning electron microscopy (sem).

To determine the dominant corrosion mechanism, electrochemical impendence was performed in a potential of 10 mv and a frequency range of 0.01-10 khz.

RESULTS AND DISCUSSIONS

The hardness results of AZ91 samples are shown in Fig. 1. As can be seen, by increasing the applied deformation at different loading directions, the hardness increased from 74 to 86 HV associated with three-directional forged samples. The increase in the sample hardness after applying hot plastic deformation can be originated from compressive residual stress and the increase in the number of twinnings and dislocations, which prevented penetration of the indenter in the sample surface. However, Ebrahimi et al.[37] reported that in accordance to equation (2) dynamic recrystallization phenomenon as a dominant mechanism occurred during hot deformation of AZ91 alloy, which reduced the average of grain size and in consequence enhanced the hardness of the alloy based on Hall-Petch equation (equation (3))[38].

$$X_{DRX} = 1 - exp\left[-0.3\left(\frac{\varepsilon-\varepsilon_c}{\varepsilon_p}\right)^{\acute{m}}\right] \quad (2)$$

$$\sigma_d = \sigma_0 + \frac{K_{HP}}{\sqrt{d}} \quad (3)$$

Where XDRX is dynamic recrystallization fraction, εc is a critical strain, εp is strain peak, m′ is constant of the material, σd is ultimate stress, σ0 is a frictional strain, d is grain size, and KHP is a constant integer.

Future Generation of Communication and Internet of Things (FGCIOT)

Journal homepage: http://fgciot.semnaniau.ac.ir/

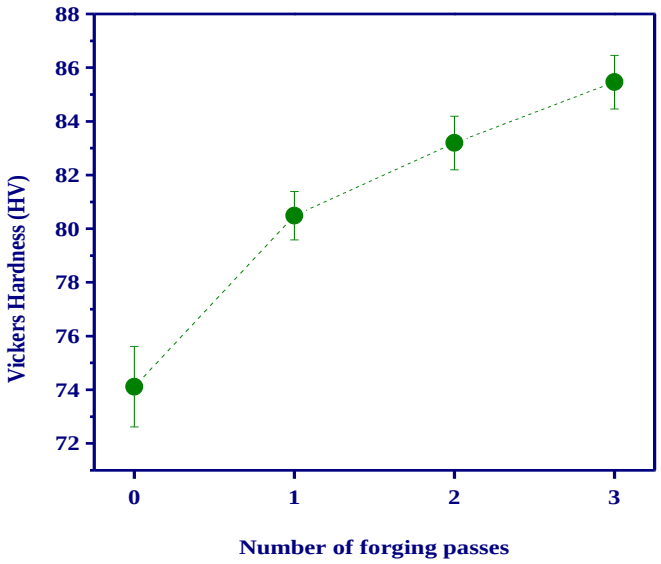

Fig. 1: Vickers hardness of AZ91 samples before and after applying the forging process

In Fig. 2, the results of optical microscopy are shown. By increasing the mechanical deformation, the grain size is reduced and anodic zones have lower distribution with thicker size. In as-received sample,narrow grain-boundaries have clearly separated all grains, but with increased plastic deformation, the grains have become finer and the separation of grain is difficult.

The results of the potentiodynamic polarization of the AZ91 samples before and after applying deformation in different directions are indicated in Fig. 3. It can be seen that applying mechanical work decreased corrosion potential and current of the samples. By determining Tafel slope from data obtained in Fig. 4, it can be concluded that the corrosion potential of as-cast samples, which was about -1.84 V, decreased to -1.26 V (compared to the saturated calomel electrode (SCE)) by applying continual three-directional forging. Although it is expected that the intensity of corrosion caused by rising of strain energy increases by increasing deformation and as a consequence residual stress in the samples, the obtained controversial results indicated that the dominant corrosion mechanism after deformation was inhomogeneous corrosion. So, the results confirmed that by applying stress and compressive deformation, grain size was reduced, sub-grains were formed, and casting voids and cracks were eliminated.The events, in consequence, caused a reduction in the active anode surface compared to the protected cathode surface. Hence, the effective contact surface with the corrosive solution and accessible anode surface that provide the required corrosion electron were limited.

Fig. 5 shows the SEM micrographs of the AZ91 samples influenced by potentiodynamic polarization deformation in a 3.5% NaCl solution. It is observed in Fig. 4-a that homogenous corrosion occurred on the most surface of the sample, and corrosion has been clearly recognizable around grain boundaries, voids and cracks. In Fig. 5b-d is observed that by applying plastic deformation in different directions, the dominant corrosion mechanism transferred to crevice corrosion and most of the destruction occurred around grain boundaries. In the research performed by Kovaci et al.[39] about the corrosion mechanism of a severe plastic deformed low-alloyed steel, the same behavior was reported. They described that transferring from homogenous corrosion to localized corrosion originated from increasing energy in eligible regions including grain boundaries and cracks caused chemical destabilization in these regions. These regions played a role of localized anode regions that protected other regions. On the other hand, because of the presence of residual stress in the deformed samples, the cracks were blocked, and the diffusion of the solution which was limited, decreased the corrosion intensity of the samples.

Doi:

Future Generation of Communication and Internet of Things (FGCIOT)

Journal homepage: http://fgciot.semnaniau.ac.ir/

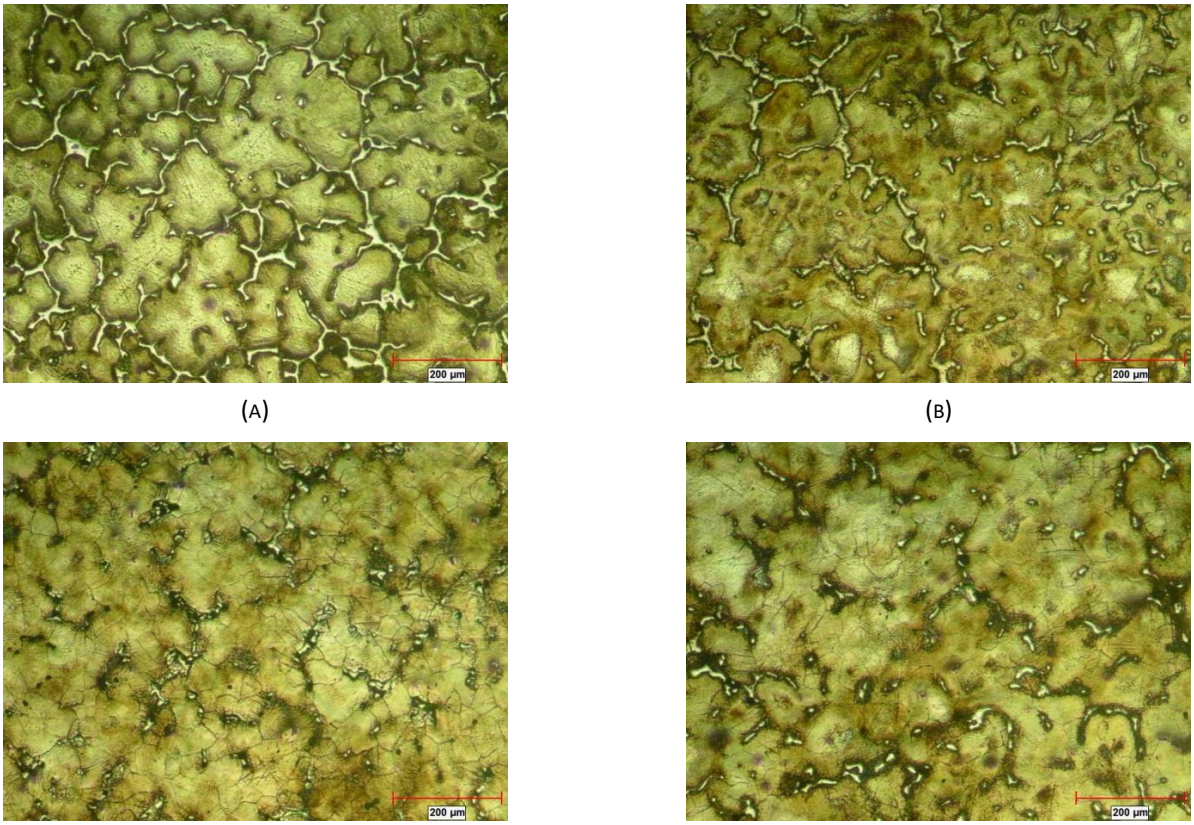

(A) (B)

(C) (d)

Fig. 2- The results of optical microscopy of AZ91 alloy, a) as-received, b) 1pass, c) 2 passes, d) 3 passes forged.

Doi:

Future Generation of Communication and Internet of Things (FGCIOT)

Journal homepage: http://fgciot.semnaniau.ac.ir/

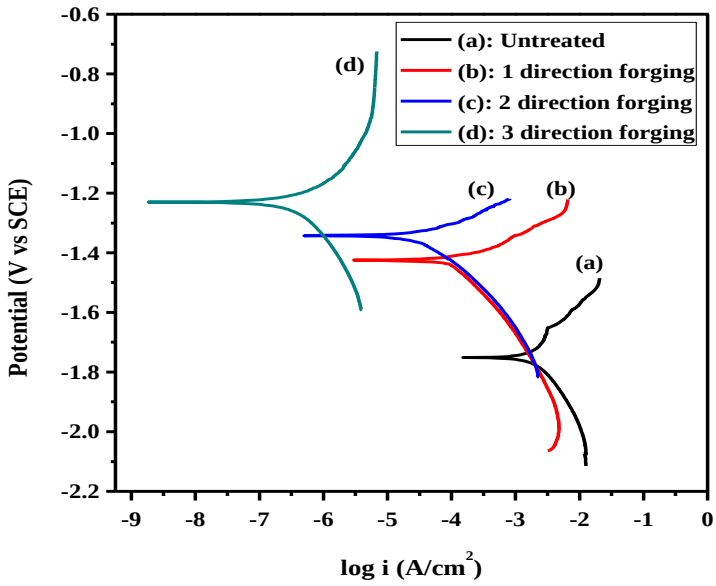

Fig. 3The results of potentiodynamic polarization of AZ91 samples after casting and deformation in different directions.

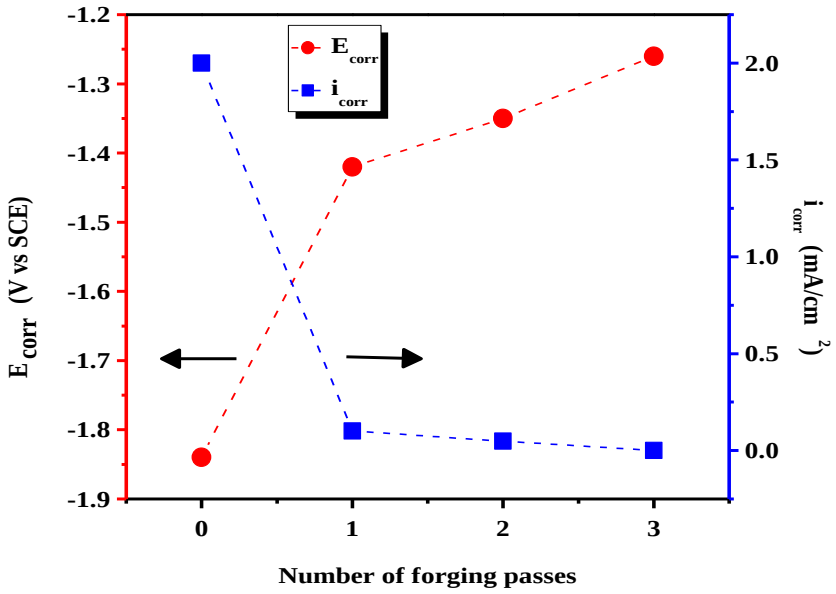

Fig.4 The results of measured Tofel slope of AZ91 samples before and after applying mechanical deformation.

Doi:

Future Generation of Communication and Internet of Things (FGCIOT)

Journal homepage: http://fgciot.semnaniau.ac.ir/

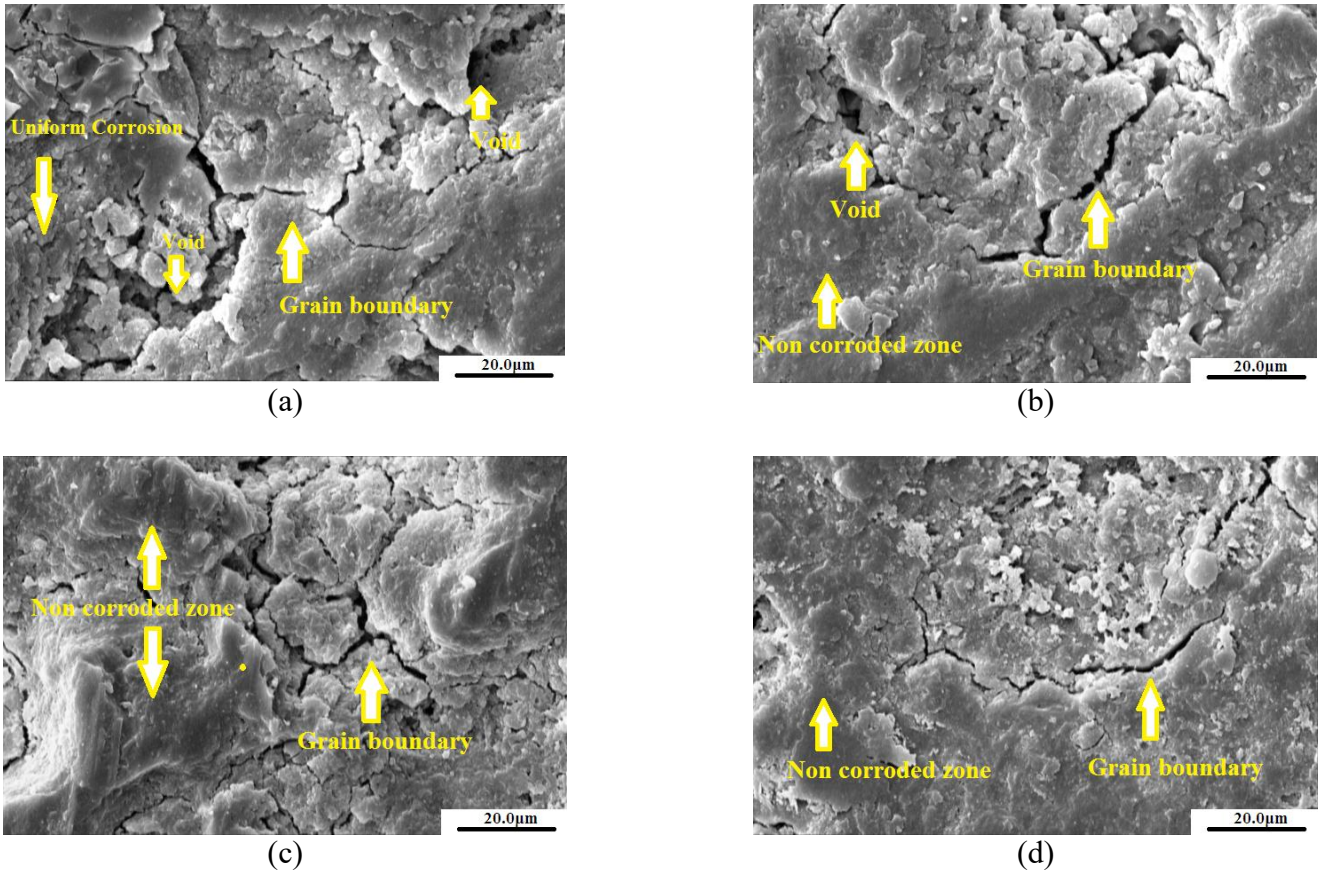

Fig. 5 The scanning electron microscopic images of corroded surface of AZ91 samples after the potentiodynamic polarization test in 3.5% NaCl solution, a) as-cast b) deformed in one direction, b) deformed in two consecutive directions, and c) deformed in three consecutive directions.

The results obtained from electrochemical impedance spectroscopy (EIS) have been indicated in Fig. 6. It is observed that applying the forging procedure and increasing the deformation directions increased the capacitive circle. The biggest capacitive circle was found in the sample forged in three directions. The evaluation of the sample via potentiodynamic polarization and SEM showed that it possessed the highest corrosion resistance, and the corrosion was limited to grain boundaries, and the voids were not observed in the corroded regions. The increase in the circle of EIS graph can be originated from the complete elimination of voids by applying three-directional deformation, which prevented the diffusion of the corrosive solution in the alloy and improved its corrosion resistance.

Randles equivalent circuit of EIS tests is indicated in Fig. 7. In the circuit, Ru is solution resistance, Cf is phase constant, and RP is polarization resistance. According to the results, RP was influenced by the intensity of deformation and increased from 381.99 Ω.cm2, related to the as-cast sample, to 1914.4 Ω.cm2, associated with the three-directional deformed sample. The event

Doi:

showed that by applying deformation, polarization resistance increased and corrosion rate decreased. The obtained results confirmed the positive effect of grain size reduction, compressive strain formation, and blocking of the presented microcracks on corrosion behavior of the alloy.

On the other hand, it was observed that capacitive behavior (Cf), which is the indication of double layer formation on the sample surface, was reduced by applying a deformation pass to the as-cast sample and by applying more passes the behavior increased. The first reduction of double layer capacity resulted from the dominated effect of residual stress on the alloy surface that destabilized the capacitive behavior of the layer. However, applying more forging pass in different directions reduced the grain sizes and blocked more microcracks, which caused the increase of double layer capacity.

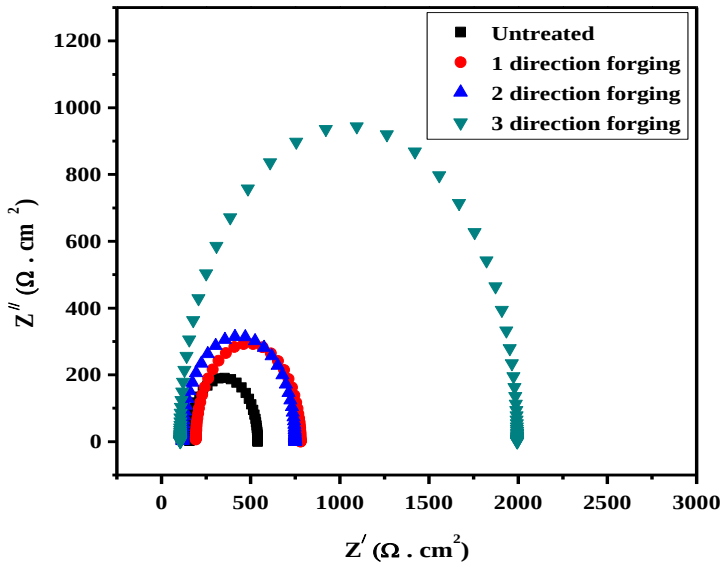

Fig. 6 Simulated Nyquist plot obtained from electrochemical impedance test of AZ91 samples before and after applying the forging process.

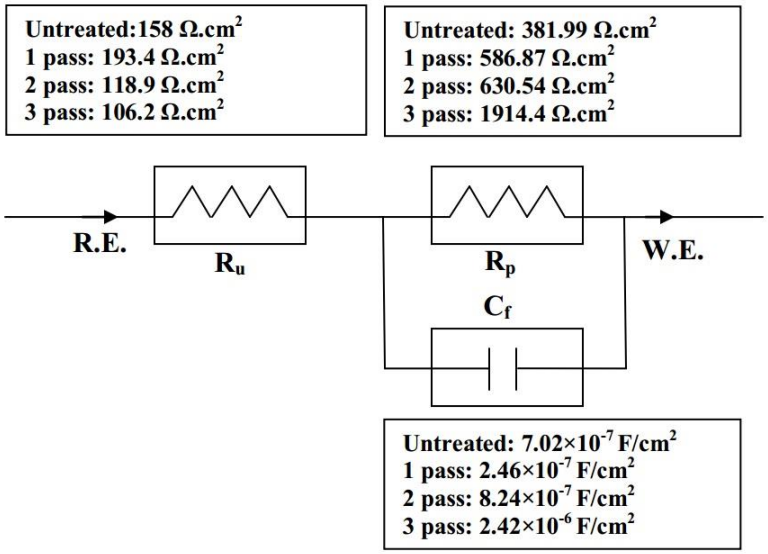

Fig. 7 Randles circuit obtained from electrochemical impedance test of AZ91 samples before and after applying the forging process.

Future Generation of Communication and Internet of Things (FGCIOT)

Journal homepage: http://fgciot.semnaniau.ac.ir/

CONCLUSIONS

By applying severe plastic deformation on AZ91 magnesium alloy at 350 °C, the following results were obtained:

By increasing the severe plastic deformation on the samples, grain size reduced and compressive residual strain remained in the metal crystal structure. In consequence, hardness was increased that all the events can be effective on the corrosion behavior of the alloy.The results of potentiodynamic polarization indicated that by increasing the intensity of deformation, due to the reduction of anode regions on the sample surface, corrosion current decreased and corrosion potential became more positive. Besides, the microscopic evaluation of the corroded surface also confirmed the reduction of anode regions. Furthermore, the results of electrochemical impedance showed that polarization resistance of the samples increased by increasing the intensity of deformation and in consequence, corrosion resistance of the samples was improved.

References

[1] Kiahosseini, S.R., et al., Structural and corrosion characterization of hydroxyapatite/zirconium nitride-coated AZ91 magnesium alloy by ion beam sputtering. Applied Surface Science, 2017. 401: p. 172-180.

[2] Kiahosseini, S.R., et al., Electrochemical evaluation of hydroxyapatite/ZrN coated magnesium biodegradable alloy in Ringer solution as a simulated body fluid. Journal of Chemical Health Risks, 2018. 5(1).

[3] Kiahosseini, S.R. and M.M. Larijani, Effects of nitrogen gas ratio on the structural and corrosion properties of ZrN thin films grown on biodegradable magnesium alloy by ion-beam sputtering. Applied Physics A, 2017. 123(12): p. 759.

[4] Meenashisundaram, G.K., S. Seetharaman, and M. Gupta, Enhancing overall tensile and compressive response of pure Mg using nano-TiB2 particulates. Materials Characterization, 2014. 94: p. 178-188.

[5] Rashad, M., F. Pan, and M. Asif, Room temperature mechanical properties of Mg–Cu–Al alloys synthesized using powder metallurgy method. Materials Science and Engineering: A, 2015. 644: p. 129-136.

[6] Song, G. and A. Atrens, Understanding magnesium corrosion—a framework for improved alloy performance. Advanced engineering materials, 2003. 5(12): p. 837-858.

[7] Hilpert, M. and L. Wagner, Corrosion fatigue behavior of the high-strength magnesium alloy AZ 80. Journal of materials engineering and performance, 2000. 9(4): p. 402-407.

[8] Abbott, T.B., Magnesium: industrial and research developments over the last 15 years. Corrosion, 2014. 71(2): p. 120-127.

[9] Esmaily, M., et al., Fundamentals and advances in magnesium alloy corrosion. Progress in Materials Science, 2017. 89: p. 92-193.

[10] Curioni, M., et al., Correlation between electrochemical impedance measurements and corrosion rate of magnesium investigated by real-time hydrogen measurement and optical imaging. Electrochimica Acta, 2015. 166: p. 372-384.

[11] Platts, A.T., Understanding and Simulating High Strain Rate Deformation of Magnesium WE43 Plate Products. 2019, The University of Manchester (United Kingdom).

[12] Roodposhti, P.S., et al., Effects of microstructure and processing methods on creep behavior of AZ91 magnesium alloy. Journal of Materials Engineering and Performance, 2016. 25(9): p. 3697-3709.

[13] Cano, Z., J. Kish, and J. McDermid, On the evolution of cathodic activity during corrosion of magnesium alloy AZ31B in a dilute NaCl solution. Journal of The Electrochemical Society, 2016. 163(3): p. C62-C68.

[14] Kish, J., et al., Corrosion performance of friction stir linear lap welded AM60B joints. JOM, 2017. 69(11): p. 2335-2344.

[15] Kandemir, S., Development of Graphene Nanoplatelet-Reinforced AZ91 Magnesium Alloy by Solidification Processing. Journal of Materials Engineering and Performance, 2018. 27: p. 3014-3023.

[16] Zhu, S., et al., The influence of minor Mn additions on creep resistance of die-cast Mg–Al–RE alloys. Materials Science and Engineering: A, 2017. 682: p. 535-541.

[17] Hanna, A., et al., Effect of hot rolling on the corrosion behavior of AZ31 magnesium alloy. Metallurgical Research & Technology, 2019. 116(1): p. 109.

[18] Wenwen, D., et al., Microstructure and mechanical properties of Mg–Al based alloy with calcium and rare earth additions. Materials Science and Engineering: A, 2003. 356(1-2): p. 1-7.

[19] Kumar, N.R., et al., Grain refinement in AZ91 magnesium alloy during thermomechanical processing. Materials Science and Engineering: A, 2003. 359(1-2): p. 150-157.

[20] Ebrahimi, G., et al., The effect of homogenization on microstructure and hot ductility behaviour of AZ91 magnesium alloy. Kovove Mater, 2010. 48: p. 277-284.

[21] Kocks, U. and D. Westlake, The importance of twinning for the ductility of CPH polycrystals. AIME MET SOC TRANS, 1967. 239(7): p. 1107-1109.

[22] Lei, S., et al., Study on corrosion resistance behavior and formation mechanism of Ce conversion coating on manganese. Metallurgical Research & Technology, 2021. 118(3): p. 319.

[23] Rzychoń, T., et al., Microstructural stability and creep properties of die casting Mg–4Al–4RE magnesium alloy. Materials Characterization, 2009. 60(10): p. 1107-1113.

Doi:

[24] Nie, K., et al., Effect of hot extrusion on microstructures and mechanical properties of SiC nanoparticles reinforced magnesium matrix composite. Journal of Alloys and Compounds, 2012. 512(1): p. 355-360.

[25] 25. Kiahosseini, S.R., et al., A Study on Structural, Corrosion, and Sensitization Behavior of Ultrafine and Coarse Grain 316 Stainless Steel Processed by Multiaxial Forging and Heat Treatment. Journal of Materials Engineering and Performance, 2018. 27(1): p. 271-281.

[26] Valiev, R.Z., et al., Producing bulk ultrafine-grained materials by severe plastic deformation. Jom, 2006. 58(4): p. 33-39.

[27] Figueiredo, R.B. and T.G. Langdon, Principles of grain refinement in magnesium alloys processed by equal-channel angular pressing. Journal of materials science, 2009. 44(17): p. 4758-4762.

[28] Tang, L., et al., Microstructures and tensile properties of Mg–Gd–Y–Zr alloy during multidirectional forging at 773 K. Materials & Design, 2013. 50: p. 587-596.

[29] Yang, X., et al., Effect of pass strain and temperature on recrystallisation in magnesium alloy AZ31 after interrupted cold deformation. Journal of Materials Science, 2012. 47(6): p. 2823-2830.

[30] Sakai, T., et al., Continuous dynamic recrystallization during the transient severe deformation of aluminum alloy 7475. Acta Materialia, 2009. 57(1): p. 153-162.

[31] Young, J.P., et al., Thermal microstructural stability of AZ31 magnesium after severe plastic deformation. Materials Characterization, 2015. 101: p. 9-19.

[32] Jiang, M., H. Yan, and R. Chen, Twinning, recrystallization and texture development during multi-directional impact forging in an AZ61 Mg alloy. Journal of Alloys and Compounds, 2015. 650: p. 399-409.

[33] Li, J., J. Liu, and Z. Cui, Microstructures and mechanical properties of AZ61 magnesium alloy after isothermal multidirectional forging with increasing strain rate. Materials Science and Engineering: A, 2015. 643: p. 32-36.

[34] Nie, K., et al., Multidirectional forging of AZ91 magnesium alloy and its effects on microstructures and mechanical properties. Materials Science and Engineering: A, 2015. 624: p. 157-168.

[35] Xia, X., et al., Microstructure, texture and mechanical properties of coarse-grained Mg–Gd–Y–Nd–Zr alloy processed by multidirectional forging. Journal of Alloys and Compounds, 2015. 623: p. 62-68.

[36] Fischer-Cripps, A.C., Nanoindentation testing, in Nanoindentation. 2011, Springer. p. 21-37.

[37] Ebrahimi, G., et al., Hot deformation behavior of AZ91 magnesium alloy in temperature ranging from 350 C to 425 C. Transactions of Nonferrous Metals Society of China, 2012. 22(9): p. 2066-2071.

[38] Li, Y., A.J. Bushby, and D.J. Dunstan, The Hall–Petch effect as a manifestation of the general size effect. Proceedings of the Royal Society A: Mathematical, Physical and Engineering Sciences, 2016. 472(2190): p. 20150890.

[39] Kovacı, H., et al., The effect of surface plastic deformation produced by shot peening on corrosion behavior of a low-alloy steel. Surface and Coatings Technology, 2019. 360: p. 78-86.